Mathematics

AIMS Mathematics, 10(4): 9614−9636.
DOI: 10.3934/math.2025443
Received: 15 October 2024
Revised: 27 February 2025
Accepted: 26 March 2025
Published: 25 April 2025

https://www.aimspress.com/journal/Math

Research article

Autonomous block method for uncertainty analysis in first-order real-world models using fuzzy initial value problem

Kashif Hussain[1], Ala Amourah[2,3,*], Jamal Salah[4,*], Ali Fareed Jameel[2] and Nidal Anakira[2,5]

[1] School of Quantitative Sciences, Universiti Utara Malaysia, Sintok, Kedah, Malaysia
[2] Mathematics Education Program, Faculty of Education and Arts, Sohar University, Sohar 311, Oman
[3] Jadara University Research Center, Jadara University, Irbid 21110, Jordan
[4] College of Applied and Health Sciences, A'Sharqiyah University, Post Box No. 42, Post Code No. 400 Ibra, Sultanate of Oman
[5] Applied Science Research Center. Applied Science Private University, Amman, Jordan

* **Correspondence:** Email: AAmourah@su.edu.om, damous73@yahoo.com.

Abstract: This article employs fuzzy derivatives and fuzzy differential equations (FDEs) to handle uncertainty in real-world applications. When exact answers are unavailable, numerical approaches are utilized to derive approximations for FDE. The autonomous two-step block method (TBM) with two higher fuzzy derivatives is used to discover optimum solutions to first-order FDEs with greater absolute accuracy. The technique competency is evaluated by analyzing first-order real-world models with fuzzy initial value problems (FIVPs). Using fuzzy calculus principles, we establish a novel universal fuzzification formulation of the TBM approach with the Taylor series. TBM is a convergent, zero-stable, and absolute stability region approach for solving linear and nonlinear fuzzy models, with a focus on regulating the convergence of approximate solutions. The developed method offers approximations for difficulties encountered in real life and is a transformational and workable method for solving first-order FIVPs.

Keywords: fuzzy derivative; first-order; two-step; block method; zero-stability; real-life models
Mathematics Subject Classification: 35A15, 45G15, 65H20, 49M27

1. Introduction

Differential equations (DEs) are used in various fields like physics, computer science, engineering, biology, economics, finance, chemistry, environmental science, medicine, and control systems to express the relationship between a quantity and its rate of change. Uncertain behavior in DEs refers to situations where minor adjustments can lead to radically different outcomes, often associated with chaotic behavior. Chaotic behavior is observed in physical, biological, and ecological systems, requiring sophisticated mathematical methods and numerical simulations.

DEs are useful for describing real-life problems, but unexpected conditions can create uncertainty. Fuzzy derivatives and fuzzy differential equations (FDEs) are used to address these challenges. This chapter covers real-world issues like temperature systems, SIR models, and liquid tank systems. The models exhibit fuzzy shapes and uncertain behavior, and the built block techniques numerically solve them.

In 1972, Zadeh and Chang [9] introduced fuzzy derivatives, with the Hukuhara derivative, Seikkala derivative, and generalized derivative being the main definitions. Puri and Ralescu [32], Seikkala [38], and Bede and Gal [8], respectively, further developed these derivatives. FDEs are challenging to solve accurately, so numerical approaches are used. Researchers use the crisp function of ordinary differential equations (ODEs) with parametric fuzzy numbers as an initial condition, focusing on lower and upper bounds. The basic fuzzy definitions, suggestions, and notions, including fuzzy sets, functions, operations, derivatives, and Zadeh extension theory, can be easily retrieved from the literature, e.g., Hashim et al. [11], Rajkumar and Rubanraj [34], Keshavarz et al. [24], and Babakordi and Allahviranloo [7].

Ma et al. [25] provided numerical solutions to first-order FDEs with FIVPs using the Euler technique. Later, researchers such as Shokri [40], Jayakumar and Kanakarajan [22], Smita and Chakraverty [41], and Najafi et al. [28] investigated alterations to the traditional Euler technique. They used triangular and trapezoidal fuzzy numbers to solve first-order linear and nonlinear FIVPs, comparing their accuracy in terms of error. Sevindir and Cetinkaya [39] and Ahmady et al. [5] used the standard Euler technique, the homotopy analysis method (HAM), and the Adomian decomposition approach. The Euler approach has advantages like simplicity and suitability for FIVPs, but presents drawbacks like lower accuracy and approximation error.

The predictor-corrector approach is a family of techniques used for first-order FDEs. It was developed by Allahviranloo et al. [6], Prakash and Kalaiselvi [31], and Salih [37] to improve numerical solutions of FIVPs. However, these approaches still have low absolute error accuracy. Ivaz et al. [17] proposed using fuzzy triangular numbers as initial conditions for the crisp ODE in the trapezoidal technique for the numerical solution of FIVPs. Ahmad et al. [3] and Maghool et al. [26] employed the Simpson method for further investigation.

The Runge-Kutta (RK) approach was first developed by [1] for numerically solving FDEs. The third-order RK method was developed by Kanagarajan and Sambath [23]. Jameel et al. [21] developed the fifth-order RK approach for first-order linear FIVPs. Parandin [30] and Nirmala [29] developed a second-order RK technique using trapezoidal fuzzy starting conditions for FDEs. Ahmadian et al. [4] created the fourth-order RK approach for first-order linear FIVPs. However, the RK method is generally unsuitable for solving stiff equations due to increasing iteration steps [19].

The block technique, first developed by Mehrkanoon et al. [27], is a method used for numerically solving first-order Fourier transforms (FDEs) with Fourier transforms of the polynomial (FIVPs). It was later used by Zawawi [43] in the predictor-corrector mode, completing two stages simultaneously. Ramli and Majid [35] introduced the implicit multistep block technique, which was used exclusively for linear FDEs. Fook and Ibrahim [10] developed the two-points hybrid block technique, which used the Seikkala differentiable idea for linear FDEs. Ramli and Majid [36] developed the fourth-order implicit diagonally multistep block approach, which was used for linear and nonlinear FIVPs. Isa et al. [16] presented a diagonally implicit multistep block technique of order four. The use of the approach as non-self-starting is the main flaw in the emphasized research.

In general, a variety of numerical techniques have been created to use FIVPs to solve first-order FDEs [42]. But there remain gaps in the solution, including self-starting problems and accuracy in terms of absolute error for first-order FDEs.

This study presents a TBM with fuzzy derivatives for first-order FIVPs in order to overcome the shortcomings of the previously stated numerical techniques (low solution accuracy in terms of absolute error). The convergence properties of the proposed approach, such as consistency and zero-stability, are also examined. The developed method is then used with numerical examples where the initial conditions are defined as fuzzy triangular and trapezoidal number. The improved accuracy in terms of absolute error is provided in the numerical results section.

This article provides a structured overview of fuzzy set theory, deriving the TSBM with second and third fuzzy derivatives, highlighting the proposed technique's basic properties, and considering linear and nonlinear numerical examples.

This article is organized as follows: The Taylor series technique for developing the TBM is provided in Section 2. Section 3 accounts for the presence of the second and third fuzzy H derivatives, focusing on the key features of the block technique. Section 4 analyses certain numerical problems. Section 5 concludes and summarizes this study.

2. Fuzzifications of FIVP with TBM

An ODE system can be used to depict the dynamics of real-world situations in a mathematical model. However, an ODE system cannot be utilized as a credible model because of the unexpected behavior of models, which might lead to uncertainty. FDEs are utilized to manage these circumstances [21].

Consider the first-order FIVP written as

$$D\tilde{F}(\eta) = \tilde{\Omega}(\eta, \tilde{F}(\eta)), \tilde{F}(\eta_0) = \tilde{f}_0, \tag{1}$$

Where $\tilde{\Omega}$ and $\tilde{F}$ are a fuzzy function of the crisp variable η, $D\tilde{F}(\eta)$ is an H-derivative of $\tilde{\Omega}(\eta)$, and $\tilde{F}(\eta_0)$ is a fuzzy initial value that is equal to the fuzzy number $\tilde{f}_0$. Thus, the fuzzy function $\tilde{F}$ is denoted as

$$\tilde{\underset{\alpha}{\overset{\alpha}{}}}[\tilde{F}(\eta)] = \left[\underline{\tilde{F}}(\eta,\alpha), \bar{\tilde{F}}(\eta,\alpha)\right], \alpha \in [0,1], \tag{2}$$

and the α-cuts of $\tilde{F}(\eta)$ is denoted as

$$\begin{cases} \tilde{\underset{\alpha}{\overset{\alpha}{}}}[\tilde{F}(\eta)] = \left[\underline{\tilde{F}}(\eta,\alpha), \bar{\tilde{F}}(\eta,\alpha)\right] \\ \tilde{\underset{\alpha}{\overset{\alpha}{}}}[\tilde{F}(\eta_0)] = \left[\underline{\bar{\tilde{F}}}(\eta_0,\alpha), \bar{\tilde{F}}(\eta_0,\alpha)\right] \end{cases}. \tag{3}$$

Given that the first-order FIVP of the form defined in Eq (1) is a mapping $\tilde{\Omega}: \mathbb{R}_{\tilde{\Omega}} \to \mathbb{R}_{\tilde{\Omega}}$ and $\tilde{F}_0 \in \mathbb{R}_{\tilde{\Omega}}$ with an α-level set in Eqs (2) and (3), at which point $h = \frac{t-t_0}{N}, t_n = t_0 + nh, 0 \leq n \leq N.$

The expression to develop a second and third fuzzy derivative TBM method for first-order FIVPs using the Taylor Series block approach is obtained as

$$\tilde{F}_{n+k}(\eta,\alpha) = \underset{\underline{\alpha}}{\overset{\alpha}{}}\left(\tilde{F}_n(\eta,\alpha) + \sum_{i=0}^{2}(\zeta_{ik}\tilde{\Omega}_{n+i}(\eta,\alpha) + \phi_{ik}\tilde{\lambda}_{n+i}(\eta,\alpha) + \psi_{ik}\tilde{\delta}_{n+i}(\eta,\alpha))\right), k = 1, 2\,. \tag{4}$$

Where ζ_{ik}, ϕ_{ik}, and ψ_{ik} are the coefficients of the first, second, and third derivatives, respectively. Expanding Eq (4) leads to the expression in Eq (5)

$$\left.\begin{array}{l} \tilde{F}_{n+1}(\eta,\alpha)= {}^{\alpha}_{\underline{\alpha}}\begin{pmatrix} \tilde{F}_n(\eta,\alpha)+\zeta_{01}\tilde{\Omega}_n(\eta,\alpha)+\zeta_{11}\tilde{\Omega}_{n+1}(\eta,\alpha)+\zeta_{21}\tilde{\Omega}_{n+2}(\eta,\alpha)+\phi_{01}\tilde{\lambda}_n(\eta,\alpha)+ \\ \phi_{11}\tilde{\lambda}_{n+1}(\eta,\alpha)+\phi_{21}\tilde{\lambda}_{n+2}(\eta,\alpha)+\psi_{01}\tilde{\delta}_n(\eta,\alpha)+\psi_{11}\tilde{\delta}_{n+1}(\eta,\alpha)+\psi_{21}\tilde{\delta}_{n+2}(\eta,\alpha) \end{pmatrix} \\ \tilde{F}_{n+2}(\eta,\alpha)= {}^{\alpha}_{\underline{\alpha}}\begin{pmatrix} \tilde{F}_n(\eta,\alpha)+\zeta_{02}\tilde{\Omega}_n(\eta,\alpha)+\zeta_{12}\tilde{\Omega}_{n+1}(\eta,\alpha)+\zeta_{22}\tilde{\Omega}_{n+2}(\eta,\alpha)+\phi_{02}\tilde{\lambda}_n(\eta,\alpha)+ \\ \phi_{12}\tilde{\lambda}_{n+1}(\eta,\alpha)+\phi_{22}\tilde{\lambda}_{n+2}(\eta,\alpha)+\psi_{02}\tilde{\delta}_n(\eta,\alpha)+\psi_{12}\tilde{\delta}_{n+1}(\eta,\alpha)+\psi_{22}\tilde{\delta}_{n+2}(\eta,\alpha) \end{pmatrix} \end{array}\right]. \tag{5}$$

Expanding the individual term in Eq (5) by applying a Taylor series expansion in fuzzy form as

$$\tilde{F}_n={}^{\alpha}_{\underline{\alpha}}\left(\tilde{F}(\eta_n,\alpha)\right),\tilde{\Omega}_n={}^{\alpha}_{\underline{\alpha}}\left(\tilde{F}'(\eta_n,\alpha)\right),\tilde{\lambda}_n={}^{\alpha}_{\underline{\alpha}}\left(\tilde{F}''(\eta_n,\alpha)\right),\tilde{\delta}_n={}^{\alpha}_{\underline{\alpha}}\left(\tilde{F}'''(\eta_n,\alpha)\right)$$

$$\tilde{F}_{n+1}=\tilde{F}(h;\eta_n,\alpha)={}^{\alpha}_{\underline{\alpha}}\left(\tilde{F}(\eta_n,\alpha)+h\tilde{F}'(\eta_n,\alpha)+\tilde{F}''(\eta_n,\alpha)\tfrac{(h)^2}{2!}+\tilde{F}'''(\eta_n,\alpha)\tfrac{(h)^3}{3!}+\ldots+\tilde{F}^{(n)}(\eta_n,\alpha)\tfrac{(h)^n}{n!}\right)$$

$$\tilde{F}_{n+2}=\tilde{F}(h;\eta_n,\alpha)={}^{\alpha}_{\underline{\alpha}}\left(\tilde{F}(\eta_n,\alpha)+2h\tilde{F}'(\eta_n,\alpha)+\tilde{F}''(\eta_n,\alpha)\tfrac{(2h)^2}{2!}+\tilde{F}'''(\eta_n,\alpha)\tfrac{(2h)^3}{3!}+\ldots+\tilde{F}^{(n)}(\eta_n,\alpha)\tfrac{(2h)^n}{n!}\right)$$

$$\tilde{\Omega}_{n+1}=\tilde{\Omega}(h;\eta_n,\alpha)={}^{\alpha}_{\underline{\alpha}}\left(\tilde{F}'(\eta_n,\alpha)+h\tilde{F}''(\eta_n,\alpha)+\tilde{F}'''(\eta_n,\alpha)\tfrac{(h)^2}{2!}+\tilde{F}^{(iv)}(\eta_n,\alpha)\tfrac{(h)^3}{3!}+\ldots+\tilde{F}^{(n)}(\eta_n,\alpha)\tfrac{(h)^n}{n!}\right)$$

$$\tilde{\Omega}_{n+2}=\tilde{\Omega}(2h;\eta_n,\alpha)={}^{\alpha}_{\underline{\alpha}}\left(\tilde{F}'(\eta_n,\alpha)+2h\tilde{F}''(\eta_n,\alpha)+\tilde{F}'''(\eta_n,\alpha)\tfrac{(2h)^2}{2!}+\tilde{F}^{(iv)}(\eta_n,\alpha)\tfrac{(2h)^3}{3!}+\ldots+\tilde{F}^{(n)}(\eta_n,\alpha)\tfrac{(2h)^n}{n!}\right)$$

$$\tilde{\lambda}_{n+1}=\tilde{\lambda}(h;\eta_n,\alpha)={}^{\alpha}_{\underline{\alpha}}\left(\tilde{F}''(\eta_n,\alpha)+h\tilde{F}'''(\eta_n,\alpha)+\tilde{F}^{(iv)}(\eta_n,\alpha)\tfrac{(h)^2}{2!}+\tilde{F}^{(v)}(\eta_n,\alpha)\tfrac{(h)^3}{3!}+\ldots+\tilde{F}^{(n)}(\eta_n,\alpha)\tfrac{(h)^n}{n!}\right)$$

$$\tilde{\lambda}_{n+2}=\tilde{\lambda}(2h;\eta_n,\alpha)={}^{\alpha}_{\underline{\alpha}}\left(\tilde{F}''(\eta_n,\alpha)+2h\tilde{F}'''(\eta_n,\alpha)+\tilde{F}^{(iv)}(\eta_n,\alpha)\tfrac{(2h)^2}{2!}+\tilde{F}^{(v)}(\eta_n,\alpha)\tfrac{(2h)^3}{3!}+\ldots+\tilde{F}^{(n)}(\eta_n,\alpha)\tfrac{(2h)^n}{n!}\right)$$

$$\tilde{\delta}_{n+1}=\tilde{\delta}(h;\eta_n,\alpha)={}^{\alpha}_{\underline{\alpha}}\left(\tilde{F}'''(\eta_n,\alpha)+h\tilde{F}^{(iv)}(\eta_n,\alpha)+\tilde{F}^{(v)}(\eta_n,\alpha)\tfrac{(h)^2}{2!}+\tilde{F}^{(v)}(\eta_n,\alpha)\tfrac{(h)^3}{3!}+\ldots+\tilde{F}^{(n)}(\eta_n,\alpha)\tfrac{(h)^n}{n!}\right)$$

$$\tilde{\delta}_{n+2}=\tilde{\delta}(2h;\eta_n,\alpha)={}^{\alpha}_{\underline{\alpha}}\left(\tilde{F}'''(\eta_n,\alpha)+2h\tilde{F}^{(iv)}(\eta_n,\alpha)+\tilde{F}^{(v)}(\eta_n,\alpha)\tfrac{(2h)^2}{2!}+\tilde{F}^{(v)}(\eta_n,\alpha)\tfrac{(2h)^3}{3!}+\ldots+\tilde{F}'''^{(n)}(\eta_n,\alpha)\tfrac{(2h)^n}{n!}\right).$$

Put these above values in Eq (5) and we obtain the expression below as

$${}^{\alpha}_{\underline{\alpha}}\left(\begin{array}{l} \tilde{F}(\eta_n,\alpha)+h\tilde{F}'(\eta_n,\alpha)+\tilde{F}''(\eta_n,\alpha)\tfrac{(h)^2}{2!}+\tilde{F}'''(\eta_n,\alpha)\tfrac{(h)^3}{3!}+\ldots+\tilde{F}^{(n)}(\eta_n,\alpha)\tfrac{(h)^n}{n!}-\tilde{F}(\eta_n,\alpha)-\zeta_{01}\tilde{F}'(\eta_n,\alpha) \\ -\zeta_{11}(\tilde{F}'(\eta_n,\alpha)+h\tilde{F}''(\eta_n,\alpha)+\tilde{F}'''(\eta_n,\alpha)\tfrac{(h)^2}{2!}+\tilde{F}^{(iv)}(\eta_n,\alpha)\tfrac{(h)^3}{3!}+\ldots+\tilde{F}^{(n)}(\eta_n,\alpha)\tfrac{(h)^n}{n!})-\zeta_{21}(\tilde{F}'(\eta_n,\alpha)+ \\ 2h\tilde{F}''(\eta_n,\alpha)+\tilde{F}'''(\eta_n,\alpha)\tfrac{(2h)^2}{2!}+\tilde{F}^{(iv)}(\eta_n,\alpha)\tfrac{(2h)^3}{3!}+\ldots+\tilde{F}^{(n)}(\eta_n,\alpha)\tfrac{(2h)^n}{n!})-\phi_{01}\tilde{F}''(\eta_n,\alpha)-\phi_{11}(\tilde{F}''(\eta_n,\alpha) \\ +h\tilde{F}'''(\eta_n,\alpha)+\tilde{F}^{(iv)}(\eta_n,\alpha)\tfrac{(h)^2}{2!}+\tilde{F}^{(v)}(\eta_n,\alpha)\tfrac{(h)^3}{3!}+\ldots+\tilde{F}^{(n)}(\eta_n,\alpha)\tfrac{(h)^n}{n!})-\phi_{21}(\tilde{F}''(\eta_n,\alpha)+2h\tilde{F}'''(\eta_n,\alpha) \\ +\tilde{F}^{(iv)}(\eta_n,\alpha)\tfrac{(2h)^2}{2!}+\tilde{F}^{(v)}(\eta_n,\alpha)\tfrac{(2h)^3}{3!}+\ldots+\tilde{F}^{(n)}(\eta_n,\alpha)\tfrac{(2h)^n}{n!})-\psi_{01}\tilde{F}'''(\eta_n,\alpha)-\psi_{11}(\tilde{F}'''(\eta_n,\alpha)+ \\ h\tilde{F}^{(iv)}(\eta_n,\alpha)+\tilde{F}^{(v)}(\eta_n,\alpha)\tfrac{(h)^2}{2!}+\tilde{F}^{(v)}(\eta_n,\alpha)\tfrac{(h)^3}{3!}+\ldots+\tilde{F}'''^{(n)}(\eta_n,\alpha)\tfrac{(h)^n}{n!})-\psi_{21}(\tilde{F}'''(\eta_n,\alpha)+ \\ 2h\tilde{F}^{(iv)}(\eta_n,\alpha)+\tilde{F}^{(v)}(\eta_n,\alpha)\tfrac{(2h)^2}{2!}+\tilde{F}^{(v)}(\eta_n,\alpha)\tfrac{(2h)^3}{3!}+\ldots+\tilde{F}'''^{(n)}(\eta_n,\alpha)\tfrac{(2h)^n}{n!})=0 \end{array}\right)$$

$$\left.\begin{pmatrix} \tilde{F}(\eta_n,\alpha)+2h\tilde{F}'(\eta_n,\alpha)+\tilde{F}''(\eta_n,\alpha)\frac{(2h)^2}{2!}+\tilde{F}'''(\eta_n,\alpha)\frac{(2h)^3}{3!}+\ldots+\tilde{F}^{(n)}(\eta_n,\alpha)\frac{(2h)^n}{n!}-\tilde{F}(\eta_n,\alpha)- \\ \zeta_{02}\tilde{F}'(\eta_n,\alpha)-\zeta_{12}(\tilde{F}'(\eta_n,\alpha)+h\tilde{F}''(\eta_n,\alpha)+\tilde{F}'''(\eta_n,\alpha)\frac{(h)^2}{2!}+\tilde{F}^{(iv)}(\eta_n,\alpha)\frac{(h)^3}{3!}+\ldots+\tilde{F}^{(n)}(\eta_n,\alpha)\frac{(h)^n}{n!}) \\ -\zeta_{22}(\tilde{F}'(\eta_n,\alpha)+2h\tilde{F}''(\eta_n,\alpha)+\tilde{F}'''(\eta_n,\alpha)\frac{(2h)^2}{2!}+\tilde{F}^{(iv)}(\eta_n,\alpha)\frac{(2h)^3}{3!}+\ldots+\tilde{F}^{(n)}(\eta_n,\alpha)\frac{(2h)^n}{n!})- \\ \phi_{02}\tilde{F}''(\eta_n,\alpha)-\phi_{12}(\tilde{F}''(\eta_n,\alpha)+h\tilde{F}'''(\eta_n,\alpha)+\tilde{F}^{(iv)}(\eta_n,\alpha)\frac{(h)^2}{2!}+\tilde{F}^{(v)}(\eta_n,\alpha)\frac{(h)^3}{3!}+\ldots+\tilde{F}^{(n)}(\eta_n,\alpha)\frac{(h)^n}{n!}) \\ -\phi_{22}(\tilde{F}''(\eta_n,\alpha)+2h\tilde{F}'''(\eta_n,\alpha)+\tilde{F}^{(iv)}(\eta_n,\alpha)\frac{(2h)^2}{2!}+\tilde{F}^{(v)}(\eta_n,\alpha)\frac{(2h)^3}{3!}+\ldots+\tilde{F}^{(n)}(\eta_n,\alpha)\frac{(2h)^n}{n!})- \\ \psi_{02}\tilde{F}'''(\eta_n,\alpha)-\psi_{12}(\tilde{F}'''(\eta_n,\alpha)+h\tilde{F}^{(iv)}(\eta_n,\alpha)+\tilde{F}^{(v)}(\eta_n,\alpha)\frac{(h)^2}{2!}+\tilde{F}^{(v)}(\eta_n,\alpha)\frac{(h)^3}{3!}+\ldots+\tilde{F}'''^{(n)}(\eta_n,\alpha) \\ \frac{(h)^n}{n!})-\psi_{22}(\tilde{F}'''(\eta_n,\alpha)+2h\tilde{F}^{(iv)}(\eta_n,\alpha)+\tilde{F}^{(v)}(\eta_n,\alpha)\frac{(2h)^2}{2!}+\tilde{F}^{(v)}(\eta_n,\alpha)\frac{(2h)^3}{3!}+\ldots+\tilde{F}'''^{(n)}(\eta_n,\alpha)\frac{(2h)^n}{n!})=0 \end{pmatrix}_{\underline{\alpha}}^{\alpha}.$$

Rewriting in matrix form by equating coefficients of $\tilde{F}^{(n)}(\eta_n;\alpha)$, the values of the coefficients are obtained using the matrix inverse method, and the result is given below:

$$\left[\begin{pmatrix}\zeta_{01}\\ \zeta_{11}\\ \zeta_{21}\\ \phi_{01}\\ \phi_{11}\\ \phi_{21}\\ \psi_{01}\\ \psi_{11}\\ \psi_{21}\end{pmatrix}=\begin{pmatrix}\frac{5669h}{13440}\\ \frac{8192h}{13440}\\ \frac{-421h}{13440}\\ \frac{303h^2}{4480}\\ \frac{-560h^2}{4480}\\ \frac{47h^2}{4480}\\ \frac{169h^3}{40320}\\ \frac{1024h^3}{40320}\\ \frac{-41h^3}{40320}\end{pmatrix},\begin{pmatrix}\zeta_{02}\\ \zeta_{12}\\ \zeta_{22}\\ \phi_{02}\\ \phi_{12}\\ \phi_{12}\\ \psi_{02}\\ \psi_{12}\\ \psi_{22}\end{pmatrix}=\begin{pmatrix}\frac{41h}{105}\\ \frac{128h}{105}\\ \frac{41h}{105}\\ \frac{2h^2}{35}\\ 0\\ \frac{-2h^2}{35}\\ \frac{1h^3}{315}\\ \frac{16h^3}{315}\\ \frac{h^3}{315}\end{pmatrix}\right]_{\underline{\alpha}}^{\alpha}.$$

Substituting these values in Eq (5) gives the TBM with second-third derivatives as

$$\left.\begin{array}{l} \tilde{F}_{n+1}(\eta,\alpha)=\begin{pmatrix}\tilde{F}_n(\eta,\alpha)+h(\frac{5669}{13440}\tilde{\Omega}_n(\eta,\alpha)+\frac{8192}{13440}\tilde{\Omega}_{n+1}(\eta,\alpha)-\frac{421}{13440}\tilde{\Omega}_{n+2}(\eta,\alpha))+h^2(\frac{303}{4480}\tilde{\lambda}_n(\eta,\alpha)- \\ \frac{560}{4480}\tilde{\lambda}_{n+1}(\eta,\alpha)+\frac{47}{4480}\tilde{\lambda}_{n+2}(\eta,\alpha))+h^3(\frac{169}{40320}\tilde{\delta}_n(\eta,\alpha)+\frac{1024}{40320}\tilde{\delta}_{n+1}(\eta,\alpha)-\frac{41}{40320}\tilde{\delta}_{n+2}(\eta,\alpha))\end{pmatrix}_{\underline{\alpha}}^{\alpha} \\ \tilde{F}_{n+2}(\eta,\alpha)=\begin{pmatrix}\tilde{F}_n(\eta,\alpha)+h(\frac{41}{105}\tilde{\Omega}_n(\eta,\alpha)+\frac{128}{105}\tilde{\Omega}_{n+1}(\eta,\alpha)+\frac{41}{105}\tilde{\Omega}_{n+2}(\eta,\alpha))+h^2(\frac{2}{35}\tilde{\lambda}_n(\eta,\alpha)- \\ \frac{2}{35}\tilde{\lambda}_{n+2}(\eta,\alpha))+h^3(\frac{1}{315}\tilde{\delta}_n(\eta,\alpha)+\frac{16}{315}\tilde{\delta}_{n+1}(\eta,\alpha)+\frac{1}{315}\tilde{\delta}_{n+2}(\eta,\alpha))\end{pmatrix}_{\underline{\alpha}}^{\alpha}\end{array}\right].$$

(6)

Following Hussain [13], the correctors of the block method in Eq (6) take the form

$$\left(A^0\tilde{F}_{n+1}=A^1\tilde{F}_{n-1}+h(C^0\tilde{\Omega}_{n-1}+C^1\tilde{\Omega}_{n+1})+h^2(D^0\tilde{\lambda}_{n-1}+D^1\tilde{\lambda}_{n+1})+h^3(E^0\tilde{\delta}_{n-1}+E^1\tilde{\delta}_{n+1})\right)$$

(7)

$$
{}^{\alpha}_{\underline{\alpha}}\left[\begin{array}{l}
A^{0}=\begin{pmatrix}1 & 0\\ 0 & 1\end{pmatrix}, A^{1}=\begin{pmatrix}0 & 1\\ 0 & 1\end{pmatrix}, C^{0}=\begin{pmatrix}\frac{3192}{13440} & \frac{-421}{13440}\\ \frac{128}{105} & \frac{41}{105}\end{pmatrix}, C^{1}=\begin{pmatrix}0 & \frac{5669}{13440}\\ 0 & \frac{41}{105}\end{pmatrix}, D^{0}=\begin{pmatrix}\frac{-560}{4480} & \frac{47}{4480}\\ 0 & \frac{-2}{35}\end{pmatrix},\\
D^{1}=\begin{pmatrix}0 & \frac{303}{4480}\\ 0 & \frac{2}{35}\end{pmatrix}, E^{0}=\begin{pmatrix}\frac{1024}{40320} & \frac{-41}{40320}\\ \frac{16}{315} & \frac{1}{315}\end{pmatrix}, E^{1}=\begin{pmatrix}0 & \frac{169}{40320}\\ 0 & \frac{1}{315}\end{pmatrix}\tilde{F}_{n+k}=\begin{pmatrix}\tilde{F}_{n+1}\\ \tilde{F}_{n+2}\end{pmatrix}, \tilde{F}_{n-k}=\begin{pmatrix}\tilde{F}_{n-1}\\ \tilde{F}_{n}\end{pmatrix},\\
\tilde{\Omega}_{n+k}=\begin{pmatrix}\tilde{\Omega}_{n+1}\\ \tilde{\Omega}_{n+2}\end{pmatrix}, \tilde{\Omega}_{n-k}=\begin{pmatrix}\tilde{\Omega}_{n-1}\\ \tilde{\Omega}_{n}\end{pmatrix}, \tilde{\lambda}_{n+k}=\begin{pmatrix}\tilde{\lambda}_{n+1}\\ \tilde{\lambda}_{n+2}\end{pmatrix}, \tilde{\lambda}_{n-k}=\begin{pmatrix}\tilde{\lambda}_{n-1}\\ \tilde{\lambda}_{n}\end{pmatrix}, \tilde{\delta}_{n+k}=\begin{pmatrix}\tilde{\delta}_{n+1}\\ \tilde{\delta}_{n+2}\end{pmatrix}, \tilde{\delta}_{n-k}=\begin{pmatrix}\tilde{\delta}_{n-1}\\ \delta\end{pmatrix}.
\end{array}\right].
$$

Fuzzification is the method of converting a crisp quantity into a fuzzy quantity, and the inverse process is known as defuzzification. For defuzzification of first-order FIVPs, Eq (1) is written as

$$\left[\tilde{F}(\eta,\tilde{\Omega})\right]=\left[\underline{\tilde{F}}(\eta,\underline{\tilde{\Omega}};\alpha),\bar{\tilde{F}}(\eta,\bar{\tilde{\Omega}};\alpha)\right], \eta\in T, \alpha\in[0,1]. \tag{8}$$

Here,

$$\left\{\underline{\tilde{F}}(\eta,\underline{\tilde{\Omega}};\alpha),=F\left[\eta,\underline{\tilde{\Omega}}(\eta),\bar{\tilde{\Omega}}(\eta)\right],\bar{\tilde{F}}(\eta,\bar{\tilde{\Omega}};\alpha)=G\left[\eta,\underline{\tilde{\Omega}}(\eta),\bar{\tilde{\Omega}}(\eta)\right].\right. \tag{9}$$

Since $D\tilde{\Omega}(\eta)=\tilde{\eta}(\eta,\tilde{\Omega}(\eta))$ is a fuzzy function, and F,G are nonlinear operators with the membership degree of $F\left[\eta,\underline{\tilde{\Omega}}(\eta),\bar{\tilde{\Omega}}(\eta)\right]$ and $G\left[\eta,\underline{\tilde{\Omega}}(\eta),\bar{\tilde{\Omega}}(\eta)\right]$ defined as

$$\begin{cases}\underline{\tilde{F}}(\eta,\underline{\tilde{\Omega}};\alpha)=min\left\{\tilde{\Omega}(\eta,\mu(\eta))|\mu(\eta)\in D\tilde{F}(\eta,\underline{\tilde{\Omega}}(\eta,\alpha))\right\}\\ \bar{\tilde{F}}(\eta,\bar{\tilde{\Omega}};\alpha)=max\left\{\tilde{\Omega}(\eta,\mu(\eta))|\mu(\eta)\in D\tilde{F}(\eta,\bar{\tilde{\Omega}}(\eta,\alpha))\right\}\end{cases} \tag{10}$$

and

$$\begin{cases}\underline{\tilde{F}}(\eta,\underline{\tilde{\Omega}};\alpha)=F\left(\eta,\underline{\tilde{\Omega}}(\eta,\alpha),\bar{\tilde{\Omega}}(\eta,\alpha)\right)=F(\eta,\tilde{\Omega}(\eta,\alpha))\\ \bar{\tilde{F}}(\eta,\bar{\tilde{\Omega}};\alpha)=G\left(\eta,\underline{\tilde{\Omega}}(\eta,\alpha),\bar{\tilde{\Omega}}(\eta,\alpha)\right)=G(\eta,\tilde{\Omega}(\eta,\alpha)).\end{cases} \tag{11}$$

3. Theoretical properties of the TBM

The following properties of the developed TBM are discussed in this section: order, zero-stability, consistency, and region of absolute stability.

Order of the TBM: Following the steps in Hussain [14], to expand individual terms of the obtained TBM in Eq (6) using a Taylor series expression gives

$$
{}^{\alpha}_{\underline{\alpha}}\left(\begin{array}{l}
\tilde{F}(\eta_n,\alpha)+h\tilde{F}'(\eta_n,\alpha)+\tilde{F}''(\eta_n,\alpha)\frac{h^2}{2!}+\tilde{F}'''(\eta_n,\alpha)\frac{h^3}{3!}+\tilde{F}^{iv}(\eta_n,\alpha)\frac{h^4}{4!}+\tilde{F}^{v}(\eta_n,\alpha)\frac{h^5}{5!}+\tilde{F}^{vi}(\eta_n,\alpha)\frac{h^6}{6!}\\
+\ldots-\tilde{F}(\eta_n,\alpha)-h(\frac{5669}{13440}\tilde{F}'(\eta_n,\alpha)+\frac{8192}{13440}(\tilde{F}'(\eta_n,\alpha)+h\tilde{F}''(\eta_n,\alpha)+\tilde{F}'''(\eta_n,\alpha)\frac{h^2}{2!}+\tilde{F}^{iv}(\eta_n,\alpha)\frac{h^3}{3!}+\\
\tilde{F}^{v}(\eta_n,\alpha)\frac{h^4}{4!}+\tilde{F}^{vi}(\eta_n,\alpha)\frac{h^5}{5!}+\ldots)-\frac{421}{13440}(\tilde{F}'(\eta_n,\alpha)+2h\tilde{F}''(\eta_n,\alpha)+\tilde{F}'''(\eta_n,\alpha)\frac{(2h)^2}{2!}+\tilde{F}^{iv}(\eta_n,\alpha)\\
\frac{(2h)^3}{3!}+\tilde{F}^{v}(\eta_n,\alpha)\frac{(2h)^4}{4!}+\tilde{F}^{vi}(\eta_n,\alpha)\frac{(2h)^5}{5!}+\ldots))-h^2(\frac{303}{4480}\tilde{F}''(\eta_n,\alpha)-\frac{560}{4480}(\tilde{F}''(\eta_n,\alpha)+h\tilde{F}'''(\eta_n,\alpha)+\\
\tilde{F}^{iv}(\eta_n,\alpha)\frac{h^2}{2!}+\tilde{F}^{v}(\eta_n,\alpha)\frac{h^3}{3!}+\tilde{F}^{vi}(\eta_n,\alpha)\frac{h^4}{4!}+\ldots)+\frac{47}{4480}(\tilde{F}''(\eta_n,\alpha)+2h\tilde{F}'''(\eta_n,\alpha)+\tilde{F}^{iv}(\eta_n,\alpha)\frac{(2h)^2}{2!}\\
+\tilde{F}^{v}(\eta_n,\alpha)\frac{(2h)^3}{3!}+\tilde{F}^{vi}(\eta_n,\alpha)\frac{(2h)^4}{4!}+\ldots))-h^3(\frac{169}{40320}\tilde{F}'''(\eta_n,\alpha)+\frac{1024}{40320}(\tilde{F}'''(\eta_n,\alpha)+h\tilde{F}^{iv}(\eta_n,\alpha)+\\
\tilde{F}^{v}(\eta_n,\alpha)\frac{h^2}{2!}+\tilde{F}^{vi}(\eta_n,\alpha)\frac{h^3}{3!}+\ldots)-\frac{41}{40320}(\tilde{F}'''(\eta_n,\alpha)+2h\tilde{F}^{iv}(\eta_n,\alpha)+\tilde{F}^{v}(\eta_n,\alpha)\frac{(2h)^2}{2!}+\ldots)=0
\end{array}\right) \tag{12}
$$

$$
\left.\begin{pmatrix}
\tilde F(\eta_n,\alpha)+2h\tilde F'(\eta_n,\alpha)+\tilde F''(\eta_n,\alpha)\frac{(2h)^2}{2!}+\tilde F'''(\eta_n,\alpha)\frac{(2h)^3}{3!}+\tilde F^{iv}(\eta_n,\alpha)\frac{(2h)^4}{4!}+\tilde F^{v}(\eta_n,\alpha)\frac{(2h)^5}{5!}+\dots) \\
-\tilde F(\eta_n,\alpha)-h(\frac{41}{105}\tilde F'(\eta_n,\alpha)+\frac{128}{105}(\tilde F'(\eta_n,\alpha)+h\tilde F''(\eta_n,\alpha)+\tilde F'''(\eta_n,\alpha)\frac{h^2}{2!}+\tilde F^{iv}(\eta_n,\alpha)\frac{h^3}{3!}+ \\
\tilde F^{v}(\eta_n,\alpha)\frac{h^4}{4!}+\dots)+\frac{41}{105}(\tilde F'(\eta_n,\alpha)+2h\tilde F''(\eta_n,\alpha)+\tilde F'''(\eta_n,\alpha)\frac{(2h)^2}{2!}+\tilde F^{iv}(\eta_n,\alpha)\frac{(2h)^3}{3!}+\tilde F^{v}(\eta_n,\alpha) \\
\frac{(2h)^4}{4!}+\dots))-h^2(\frac{2}{35}\tilde F''(\eta_n,\alpha)-\frac{2}{35}(\tilde F''(\eta_n,\alpha)+2h\tilde F'''(\eta_n,\alpha)+\tilde F^{iv}(\eta_n,\alpha)\frac{(2h)^2}{2!}+\tilde F^{v}(\eta_n,\alpha)\frac{(2h)^3}{3!} \\
+\dots))-h^3(\frac{1}{315}\tilde F'''(\eta_n,\alpha)+\frac{16}{315}(\tilde F'''(\eta_n,\alpha)+h\tilde F^{(iv)}(\eta_n,\alpha)+\tilde F^{(v)}(\eta_n,\alpha)\frac{h^2}{2!}+\dots)+\frac{1}{315}(\tilde F'''(\eta_n,\alpha)+ \\
2h\tilde F^{(iv)}(\eta_n,\alpha)+\tilde F^{(v)}(\eta_n,\alpha)\frac{(2h)^2}{2!}+\dots)=0
\end{pmatrix}^{\alpha}_{\underline{\alpha}}\right. . \quad (13)
$$

Equating the coefficients of $h^n\tilde F^{(n)}(\eta_n,\alpha)$ in Eqs (12) and (13), the order of the method is computed as

$$
\begin{pmatrix}1 & 1 & \frac{1}{2!} & \frac{1}{3!} & \frac{1}{4!} & \frac{1}{5!} & \frac{1}{6!} & \frac{1}{7!} & \frac{1}{8!} & \frac{1}{9!} & \frac{1}{10!}\end{pmatrix}^T-\begin{pmatrix}1 & 0 & 0 & 0 & 0 & 0 & 0 & 0 & 0 & 0 & 0\end{pmatrix}^T-
$$

$$
-\left[\frac{5669}{13440}\begin{pmatrix}0\\1\\0\\0\\0\\0\\0\\0\\0\\0\\0\end{pmatrix}+\frac{8192}{13440}\begin{pmatrix}0\\1\\1\\\frac{1}{2!}\\\frac{1}{3!}\\\frac{1}{4!}\\\frac{1}{5!}\\\frac{1}{6!}\\\frac{1}{7!}\\\frac{1}{8!}\\\frac{1}{9!}\end{pmatrix}-\frac{421}{13440}\begin{pmatrix}0\\1\\2\\\frac{2^2}{2!}\\\frac{2^3}{3!}\\\frac{2^4}{4!}\\\frac{2^5}{5!}\\\frac{2^6}{6!}\\\frac{2^7}{7!}\\\frac{2^8}{8!}\\\frac{2^9}{9!}\end{pmatrix}\right]-\left[\frac{303}{4480}\begin{pmatrix}0\\0\\1\\0\\0\\0\\0\\0\\0\\0\\0\end{pmatrix}-\frac{560}{4480}\begin{pmatrix}0\\0\\1\\1\\\frac{1}{2!}\\\frac{1}{3!}\\\frac{1}{4!}\\\frac{1}{5!}\\\frac{1}{6!}\\\frac{1}{7!}\\\frac{1}{8!}\end{pmatrix}-\frac{47}{4480}\begin{pmatrix}0\\0\\1\\2\\\frac{2^2}{2!}\\\frac{2^3}{3!}\\\frac{2^4}{4!}\\\frac{2^5}{5!}\\\frac{2^6}{6!}\\\frac{2^7}{7!}\\\frac{2^8}{8!}\end{pmatrix}\right]-\left[\frac{169}{40320}\begin{pmatrix}0\\0\\0\\1\\0\\0\\0\\0\\0\\0\\0\end{pmatrix}+\frac{1024}{40320}\begin{pmatrix}0\\0\\0\\1\\1\\\frac{1}{2!}\\\frac{1}{3!}\\\frac{1}{4!}\\\frac{1}{5!}\\\frac{1}{6!}\\\frac{1}{7!}\end{pmatrix}-\frac{1}{40320}\begin{pmatrix}0\\0\\0\\1\\2\\\frac{2^2}{2!}\\\frac{2^3}{3!}\\\frac{2^4}{4!}\\\frac{2^5}{5!}\\\frac{2^6}{6!}\\\frac{2^7}{7!}\end{pmatrix}\right]
$$

$$
=\begin{pmatrix}0 & 0 & 0 & 0 & 0 & 0 & 0 & 0 & 0 & 0 & 6.8893e-08\end{pmatrix}^T.
$$

And

$$
\begin{pmatrix}1 & 2 & \frac{2^2}{2!} & \frac{2^3}{3!} & \frac{2^4}{4!} & \frac{2^5}{5!} & \frac{2^6}{6!} & \frac{2^7}{7!} & \frac{2^8}{8!} & \frac{2^9}{9!} & \frac{2^{10}}{10!}\end{pmatrix}^T-\begin{pmatrix}1 & 0 & 0 & 0 & 0 & 0 & 0 & 0 & 0 & 0 & 0\end{pmatrix}^T-
$$

$$
\left[\frac{41}{105}\begin{pmatrix}0\\1\\0\\0\\0\\0\\0\\0\\0\\0\\0\end{pmatrix}+\frac{128}{105}\begin{pmatrix}0\\1\\1\\\frac{1}{2!}\\\frac{1}{3!}\\\frac{1}{4!}\\\frac{1}{5!}\\\frac{1}{6!}\\\frac{1}{7!}\\\frac{1}{8!}\\\frac{1}{9!}\end{pmatrix}+\frac{41}{105}\begin{pmatrix}0\\1\\2\\\frac{2^2}{2!}\\\frac{2^3}{3!}\\\frac{2^4}{4!}\\\frac{2^5}{5!}\\\frac{2^6}{6!}\\\frac{2^7}{7!}\\\frac{2^8}{8!}\\\frac{2^9}{9!}\end{pmatrix}\right]-\left[\frac{2}{35}\begin{pmatrix}0\\0\\1\\0\\0\\0\\0\\0\\0\\0\\0\end{pmatrix}-\frac{2}{35}\begin{pmatrix}0\\0\\1\\2\\\frac{2^2}{2!}\\\frac{2^3}{3!}\\\frac{2^4}{4!}\\\frac{2^5}{5!}\\\frac{2^6}{6!}\\\frac{2^7}{7!}\\\frac{2^8}{8!}\end{pmatrix}\right]-\left[\frac{1}{315}\begin{pmatrix}0\\0\\0\\1\\0\\0\\0\\0\\0\\0\\0\end{pmatrix}+\frac{16}{315}\begin{pmatrix}0\\0\\0\\1\\1\\\frac{1}{2!}\\\frac{1}{3!}\\\frac{1}{4!}\\\frac{1}{5!}\\\frac{1}{6!}\\\frac{1}{7!}\end{pmatrix}+\frac{1}{315}\begin{pmatrix}0\\0\\0\\1\\2\\\frac{2^2}{2!}\\\frac{2^3}{3!}\\\frac{2^4}{4!}\\\frac{2^5}{5!}\\\frac{2^6}{6!}\\\frac{2^7}{7!}\end{pmatrix}\right]=\begin{pmatrix}0\\1\\0\\0\\0\\0\\0\\0\\0\\0\\-7.6349e-09\end{pmatrix}.
$$

Thus, the order of the TBM is $q = 9$ with error constant values $C_{10} = (6.8893e-08, -7.6349e-$

$09)^T$ and principal LTE $C_7 h^{(10)} \tilde{F}^{(10)}(\eta_n, \alpha)$.

Consistency: Since the order of the TBM $q = 9 > 1$, following [15], the TBM is consistent.

Zero-stability and convergence: Following Hussain [15] to test the TBM for zero-stability, the corrector of the method is normalized according to Eq (7) to give the first characteristic polynomial $P(\phi)$ as

$$P(\phi) = det(\phi_\eta A^0 - A^1) = \Bigg|_{\underline{\alpha}}^{\alpha} \left[\begin{pmatrix} \phi & 0 \\ 0 & \phi^2 \end{pmatrix} \begin{pmatrix} 1 & 0 \\ 0 & 1 \end{pmatrix} - \begin{pmatrix} 0 & 1 \\ 0 & 1 \end{pmatrix} \right] \Bigg| = \phi(\phi^2 - 1) = 0,\ \phi = 0, \pm 1$$

which is a simple root. So, the TBM is zero-stable.

Likewise, since the TBM is consistent and zero-stable, the developed method is convergent.

Region of absolute stability: Following [13], the stability polynomial for the TBM takes the form

$$R(w) = \left|_{\underline{\alpha}}^{\alpha} \begin{matrix} -\begin{pmatrix} w & 0 \\ 0 & w^2 \end{pmatrix} + \begin{pmatrix} 0 & 1 \\ 0 & 1 \end{pmatrix}_{\underline{r}}^{\bar{r}} + q\left[\begin{pmatrix} \frac{3192w}{13440} & \frac{-421w^2}{13440} \\ \frac{128w}{105} & \frac{41w^2}{105} \end{pmatrix} + \begin{pmatrix} 0 & \frac{5669}{13440} \\ 0 & \frac{41}{105} \end{pmatrix} \right] + \\ q^2 \left[\begin{pmatrix} \frac{-560w}{4480} & \frac{47w^2}{4480} \\ 0 & \frac{-2w^2}{35} \end{pmatrix} + \begin{pmatrix} 0 & \frac{303}{4480} \\ 0 & \frac{2}{35} \end{pmatrix} \right] + q^3 \left[\begin{pmatrix} \frac{1024w}{40320} & \frac{-41w^2}{40320} \\ \frac{16w}{315} & \frac{1w^2}{315} \end{pmatrix} + \begin{pmatrix} 0 & \frac{169}{40320} \\ 0 & \frac{1}{315} \end{pmatrix} \right] \end{matrix} \right| \tag{14}$$

$$R(w) = \left(\frac{q^6}{7560} - \frac{q^5}{420} + \frac{11q^4}{504} - \frac{99161q^3}{793800} + \frac{577q^2}{1260} - \frac{33011q}{38075} + \frac{314}{315} \right) w^3 - \left(\frac{169q^6}{793800} + \frac{q^5}{304} + \frac{6287q^4}{264600} + \frac{307q^3}{2520} + \frac{11q^2}{24} + q + 1 \right) w.$$

The region of absolute stability of Eq (14) is plotted using the boundary locus approach, as shown in Figure 1.

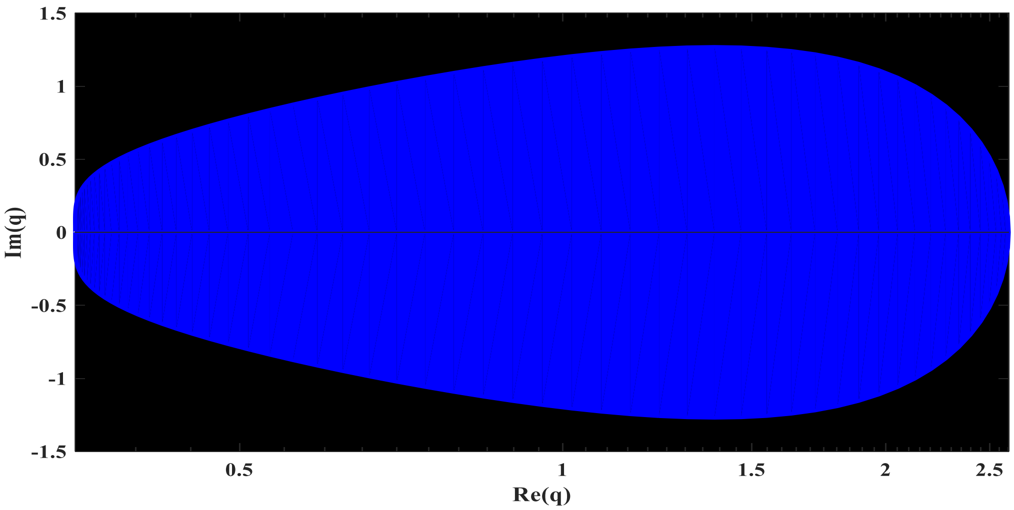

Figure 1. Interval of the absolute stability region of TBM.

Figure 1 demonstrates the interval of the stability region; also, all polynomial roots for the absolute stability region are located on the unit circle, which indicates that the large step-size h value selected can be used for the TBM.

4. Results

Implementation of the TBM for different models: The TBM is implemented by acquiring the derivatives of the supplied first-order FIVPs from numerical problems and then transforming the parameters into the α-level parametric form of fuzzy numbers. After that, the conditions $\eta_n, n = 0,1,\ldots,N$ produce two solutions $\tilde{F}(\eta_n,\alpha) = \left(\underline{\tilde{F}}(\eta_n,\alpha), \bar{\tilde{F}}(\eta_n,\alpha)\right)$, known as lower and upper solutions, respectively. To test the accuracy of the TBM developed above, the following first-order real-life models are considered.

4.1. Model 1: Logistic growth model [18]

The differential equation with fuzzy form is as follows:

$$D\tilde{F}(\eta,\alpha) = r * \tilde{F}(\eta,\alpha)(M - \tilde{F}(\eta,\alpha)). \tag{15}$$

With second-third derivatives

$D'\tilde{F}(\eta,\alpha) = r * \tilde{F}'(\eta,\alpha)(M - \tilde{F}(\eta,\alpha)) + r * \tilde{F}(\eta,\alpha)(M - \tilde{F}'(\eta,\alpha))$, and

$D''\tilde{F}(\eta,\alpha) = r * \tilde{F}''(\eta,\alpha)(M - \tilde{F}(\eta,\alpha)) + r * \tilde{F}(\eta,\alpha)(M - \tilde{F}'(\eta,\alpha)) + r * \tilde{F}'(\eta,\alpha)(M - \tilde{F}'(\eta,\alpha)$
$+ r * \tilde{F}(\eta,\alpha)(M - \tilde{F}''(\eta,\alpha))$

with positive growth constant r and carrying capacity M models' logistic growth of a quantity $\tilde{F}$ at time η with solution

$$\tilde{F}(\eta,\alpha) = \frac{M}{1+Ae^{-Mr\eta}} \text{ where } A = \frac{M-\tilde{F}_0(\eta,\alpha)}{\tilde{F}_0(\eta,\alpha)}, \text{ at } \eta = 0.$$

The initial condition is fuzzy carrying capacity $M = (500,1000,1500)$ with positive growth constant $r = 0.002$, $\tilde{F}_0(\eta,\alpha) = 1$, and $h = 0.1$. The TBM is used to the approximate solution of Eq (15) and compared with the exact solution. The solution's accuracy in terms of absolute error with lower and upper bounds is presented in Table 1 at $\eta = 8$.

Table 1. Comparison of the TBM with the exact solution for solving Model 1.

α	TBM lower approximate solution	TBM absolute error	TBM upper approximate solution	TBM absolute error
0	1.499999915116105e+03	0	4.283037321343937e+02	0
0.2	1.399999633773942e+03	0	5.766073216762441e+02	0
0.4	1.299998436035981e+03	0	6.933725626545569e+02	0
0.6	1.199993399999203e+03	0	7.982391982493232e+02	0
0.8	1.099972533921815e+03	0	8.995492413246657e+02	0
1	9.998875899978846e+02	0	9.998875899978846e+02	0

The TBM produced in this work has enhanced accuracy in terms of absolute error, as shown in Table 1. The developed TBM's three-dimensional solution for Model 1 is displayed in Figure 2. The approximate solutions, computed using the TBM, are displayed in Figures 3 and 4, with a comparison with the exact solution to illustrate the uncertain behavior of the logistic growth model for various values of α. The model in Eq (15) has a solution (membership values with α cuts) that grows with the lower bound and decreases with the upper bound, as seen in Figures 3 and 4. Furthermore, a time range was used as the initial condition of the model by using the triangular fuzzy number. This provides further details on the model's approximate solution over the initial condition.

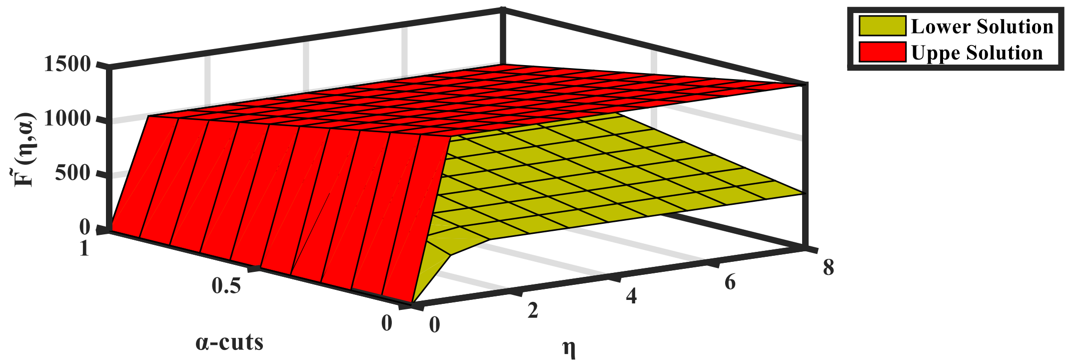

Figure 2. 3-Dimensional surface graph solution via the developed TBM for Model 1.

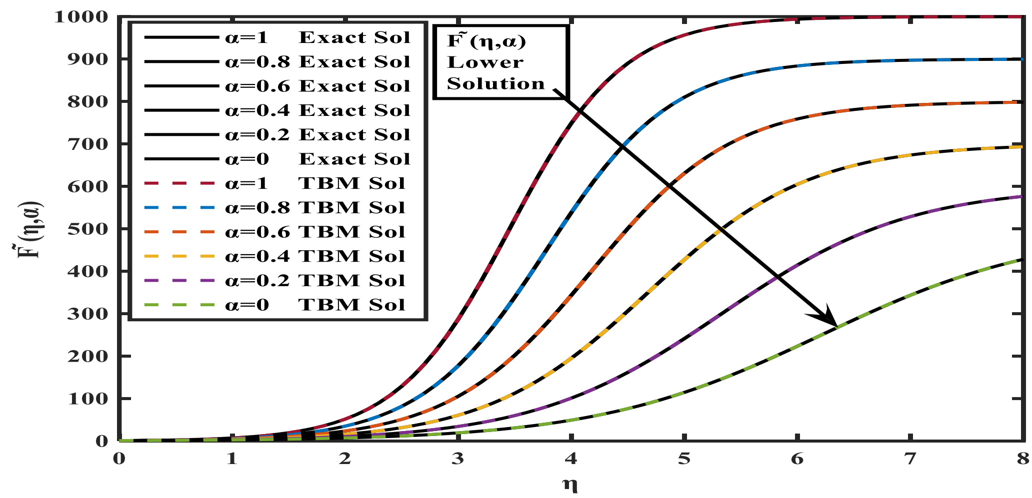

Figure 3. Uncertainty of Model 1 with α-cuts using TBM and a comparison with the exact solution.

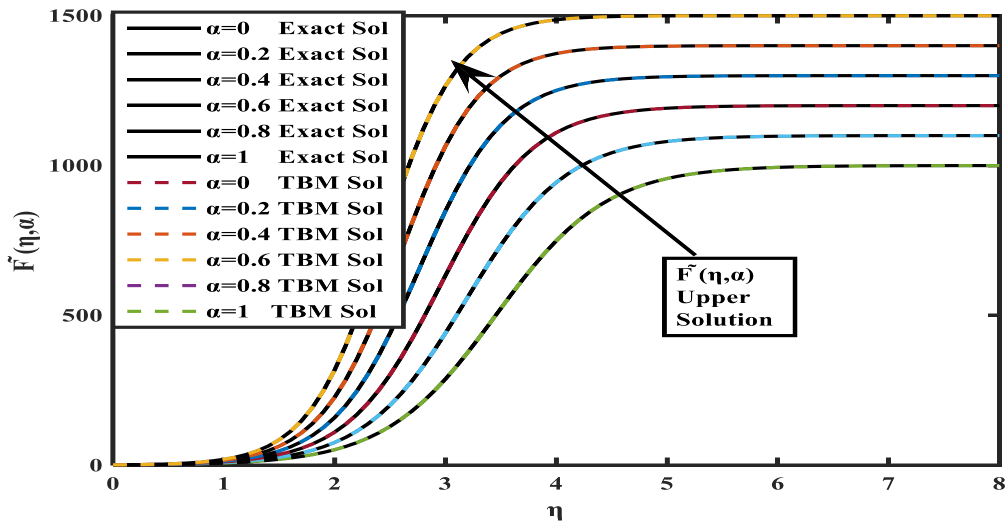

Figure 4. Uncertainty of Model 1 with α-cuts using TBM and a comparison with the exact solution.

4.2. Model 2: Thermal system [18]

Figure 5 shows a tank with a heating system.

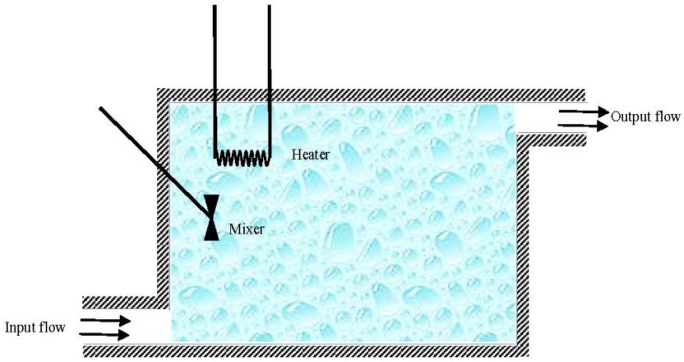

Figure 5. Thermal system.

Assume $R = 0.5$ is the flow obstruction, $C = 2$ is the thermal capacitance, and the temperature at time η is $\tilde{F}(\eta, \alpha)$. The model is

$$D\tilde{F}(\eta, \alpha) = -\frac{1}{RC}\tilde{F}(\eta, \alpha). \tag{16}$$

With second-third derivatives
$D'\tilde{F}(\eta, \alpha) = -\frac{1}{RC}D\tilde{F}(\eta, \alpha)$ and $D''\tilde{F}(\eta, \alpha) = -\frac{1}{RC}D'\tilde{F}(\eta, \alpha)$
with the initial condition $\tilde{F}(0, \alpha) = (\alpha - 1, 1 - \alpha), \alpha \in [0,1]$, and the exact solution of Eq (16) is $\tilde{F}(\eta, \alpha) = (\alpha - 1, 1 - \alpha)e^{-\eta}$ with $\eta \in [0,4]$. The TBM is used to approximate the solution of Eq (20) and is compared with the SNN and DNN methods in Jafari et al. (2017). The solution's accuracy in terms of absolute error with lower and upper bounds is presented in Table 2 at $\eta = 1$ and $h = 0.1$.

Table 2. Comparison of the TBM with Jafari et al. (2017) for solving Model 2.

α	TBM lower approximate solution	SNN absolute error	DNN absolute error	TBM absolute error
0	-367.879441171442e-03	4.0700e-02	1.8400e-02	0
0.2	-294.30355293715e-03	3.5100e-02	2.5100e-02	0
0.4	-220.72766470286e-03	3.3400e-02	1.1100e-02	0
0.6	-147.15177646857e-03	2.8200e-02	1.0400e-02	0
0.8	-73.575888234288e-03	2.5300e-02	1.0200e-02	0
1	0	3.2300e-02	1.1200e-02	0
α	TBM upper approximate solution	SNN absolute error	DNN absolute error	TBM absolute error
0	367.8794411714420e-03	6.0400e-02	3.1700e-02	2.2304e-17
0.2	294.303552937153e-03	5.7800e-02	1.0500e-02	0
0.4	220.7276647028653e-03	5.2300e-02	2.8400e-02	0
0.6	14.71517764685769e-03	4.1700e-02	3.0100e-02	0
0.8	73.57588823428849e-03	5.0100e-02	3.1300e-02	0
1	0	3.2300e-02	1.1200e-02	0

Table 2 shows the improved accuracy of the developed TBM in terms of absolute error. Figure 6 shows the 3-dimensional solution via the developed TBM for model 2. Figures 7 and 8 display the computed approximate solutions using the TBM to show the uncertain behavior of the tank thermal system with time interval [0,4] and different values of α. According to Figures 7 and 8, the solution (membership values with α-cuts) of the thermal system model in Eq (16) increases with the lower bound and decreases with the upper bound. In addition, the use of the triangular fuzzy number for the initial condition of the thermal system model was a time range of [-1,1]. This provides more information for the approximate solution of Model 2 than the initial condition.

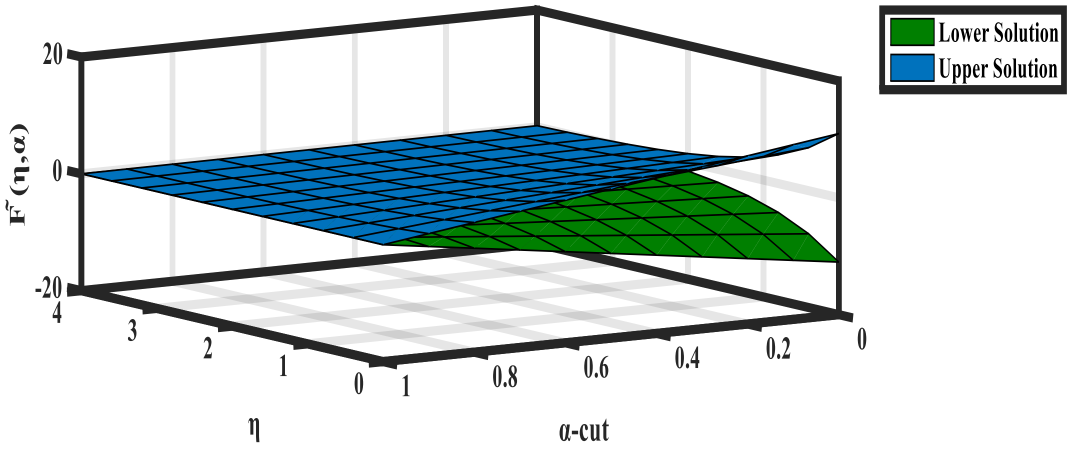

Figure 6. 3-dimensional surface graph solution via the developed TBM for Model 2.

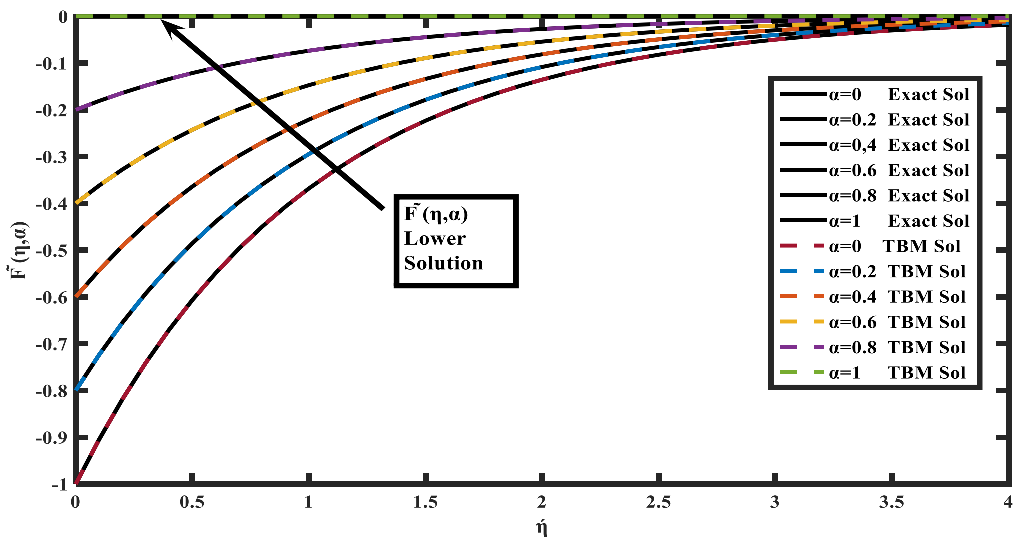

Figure 7. Uncertainty of Model 2 with α-cuts using TBM and a comparison with the exact solution.

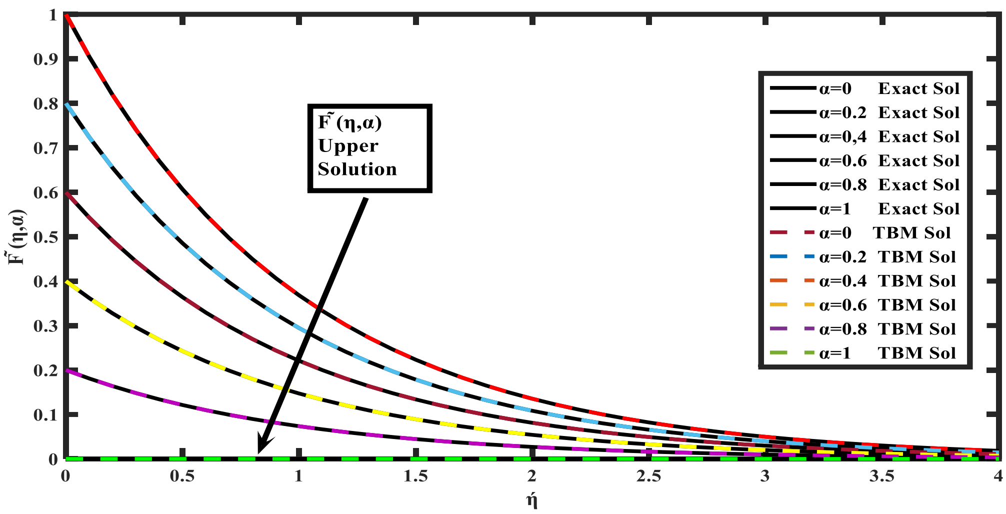

Figure 8. Uncertainty of Model 2 with α-cuts using TBM and a comparison with the exact solution.

4.3. Model 3: SIR model [2]

The potential number of individuals infected with an infectious disease over time in a closed community is calculated using the SIR model, an epidemiological model. These equations link the numbers of susceptible individuals $S(\eta)$, infected individuals$I(\eta)$, and recovered individuals $R(\eta)$, justifying the moniker of this class of models. For several infectious illnesses, such as measles, mumps, and rubella, this is an effective and basic approach. It is given by the following three coupled equations:

$$\begin{bmatrix} \frac{dS}{dt} = \mu(1-S) - \beta IS \\ \frac{dI}{dt} = \mu I - \gamma I + \beta IS \\ \frac{dR}{dt} = -\mu R + \gamma I \end{bmatrix} \tag{17}$$

where μ, β, and γ are positive parameters. Define F to be

$$F = I + S + R \tag{18}$$

the evolution equation following for F

$$F' = \mu(1-F). \tag{19}$$

Taking $\mu = 0.5$ for an initial condition (for a particular closed population). To consider uncertainty and hesitation, $\tilde{f}_0$ is a triangular intuitionistic fuzzy number. Let $\mu = 0.5$ and $\eta \in [0,1]$, $\tilde{f}_0 = (0,0.5,1)$. Then Eq (18) in fuzzy form is as follows:

$$\tilde{F}' = \mu(1-\tilde{F}). \tag{20}$$

The exact solution of Eq (20) is $\tilde{F}(\eta,\alpha) = (1-0.5\alpha, 1-(1-0.5\alpha))e^{-0.5\eta}$, $\alpha \in [0,1]$. The TBM is used to approximate the solution to Eq (20). The solution of this SIR model as a FIVP is compared with Adeyeye and Omar (2016) at α=1, where the two-step implicit Obrechkoff-type block method (2SBM) solved this model in crisp form. The solution's accuracy in terms of absolute error with lower and upper bounds is presented in Table 4 at $\eta = 1$ and $h = 0.1$.

Table 4. Comparison of the TBM with Adeyeye and Omar (2016) for solving Model 3.

α	TBM lower approximate solution	2SBM absolute error	TBM absolute error	TBM upper approximate solution	2SBM absolute error	TBM absolute error
0	1	N/A	0	393.469340e-03	N/A	0
0.2	939.34693402e-03	N/A	0	454.122406e-03	N/A	0
0.4	878.69386805e-03	N/A	0	514.775472e-03	N/A	0
0.6	818.04080208e-03	N/A	0	575.428538e-03	N/A	0
0.8	757.38773615e-03	N/A	0	636.081604e-03	N/A	0
1	696.73467014e-03	2.520e-13	0	696.734670e-03	2.5e-13	0

Table 4 shows the improved accuracy of the developed TBM in terms of absolute error. Figure 9 shows the 3-dimensional solution via the developed TBM for Model 3. Figures 10 and 11 display the computed approximate solutions using the TBM to show the uncertain behavior of the Model 3 with time interval [0,10] and different values of $\alpha \in [0,1]$. According to Figures 10 and 11, the solution (membership values with α-cuts) of the thermal system model in Eq (20) decreases with the lower bound and increases with the upper bound. In addition, the use of the triangular fuzzy number for the initial condition of the thermal system model with a range of decreases was observed for time. This provides more information for the approximate solution of the model over the initial condition.

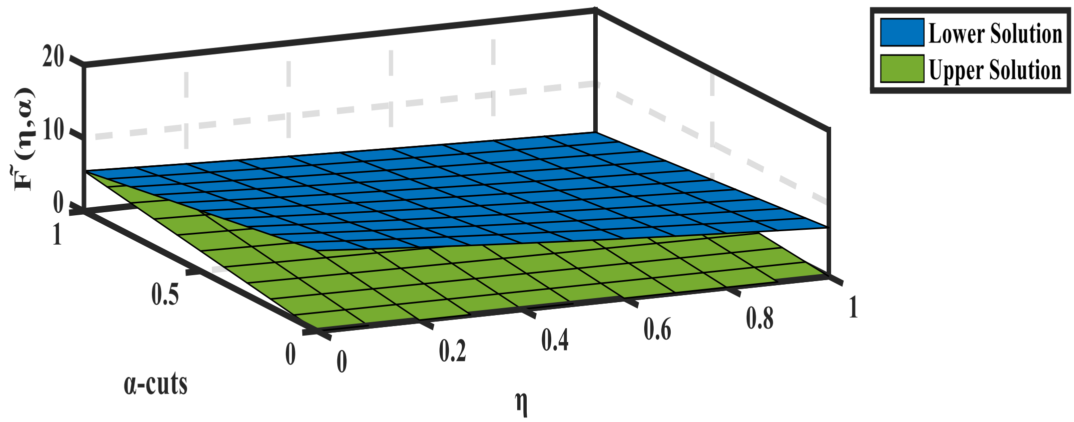

Figure 9. 3-dimensional surface graph solution via the developed TBM for Model 3.

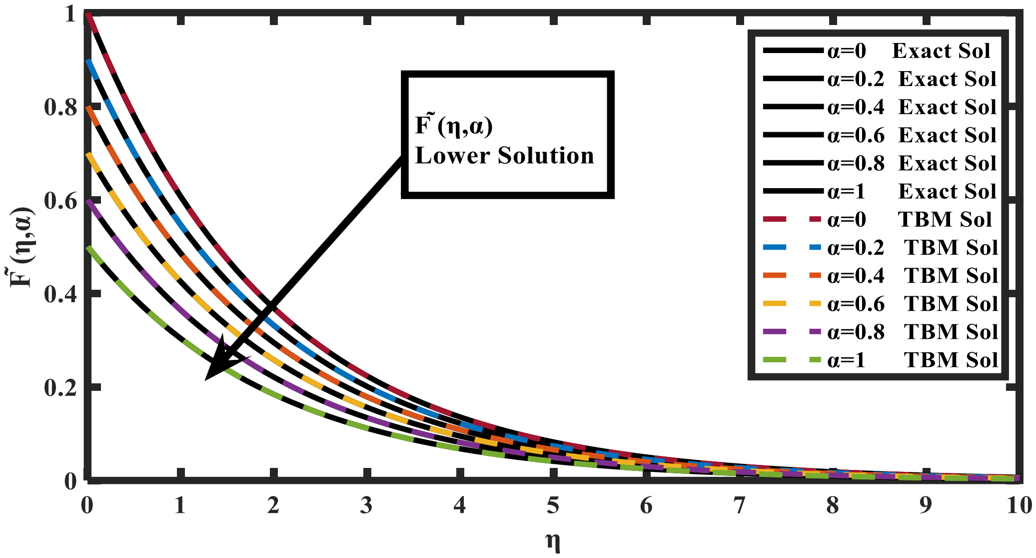

Figure 10. Uncertainty of Model 3 with α-cuts using TBM and a comparison with the exact solution.

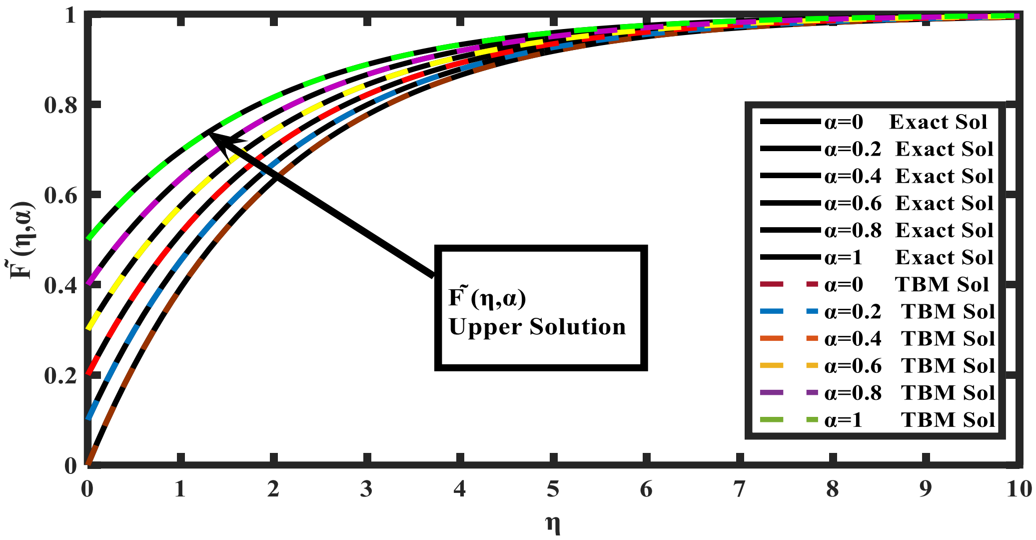

Figure 11. Uncertainty of Model 3 with α-cuts using TBM and a comparison with the exact solution.

4.4. Model 4. Charging and discharging capacitor [12]

Consider the following crisp capacitor model in Hohenauer, (2018) in fuzzy form

$$D(\widetilde{U}_c(\eta,\alpha)) = -\frac{1}{RC}\widetilde{U}_c(\eta,\alpha) + \frac{1}{RC}\widetilde{U}_G(\eta,\alpha), \tag{21}$$

with exact solution

$$\widetilde{U}_c(\eta,\alpha) = K.e^{-\int\frac{d\eta}{RC}} + \left[\int(\frac{\widetilde{U}_G(\eta,\alpha)}{RC}.e^{-\int\frac{d\eta}{RC}})dt\right].e^{-\int\frac{d\eta}{RC}}, \tag{22}$$

charging of the capacitor for the fuzzy initial condition

$$\widetilde{U}_C(0,\alpha) = \widetilde{U}_B.[1 - e^{\frac{\eta}{RC}}] \tag{23}$$

while the fuzzy initial condition discharging of the capacitor

$$\widetilde{U}_C(0,\alpha) = \widetilde{U}_{c,0}.\, e^{\frac{\eta}{RC}}. \tag{24}$$

Charging of a capacitor

The solutions are presented at $\eta = 4s$, with the triangle fuzzy number. Table 5 displays the accuracy of the bottom and upper solutions for charging a capacitor in a DC state. The resulting graphs, with battery voltage set to $12\,V, C = 0.25\,F, U_c(0) = 0$, and resistance with triangular fuzzy number $R = (2+\alpha, 4-\alpha), \alpha = [0,1]$, are displayed in Figures 13 and 14.

Discharging of a capacitor

The solutions are presented at $\eta = 4s$, with the triangle fuzzy number. Table 6 displays the accuracy of the bottom and upper solutions for discharging a capacitor in a DC state. The resulting graphs, with battery voltage set to $12\,V, C = 0.25\,F, U_c(0) = 12V$, and resistance with triangular fuzzy number $R = (2+\alpha, 4-\alpha), \alpha = [0,1]$, are displayed in Figures 16 and 17.

Table 5. Comparison of the TBM with the exact solution for solving the charging of a capacitor in Model 4.

α	TBM lower approximate solution	TBM absolute error	TBM upper approximate solution	TBM absolute error
0	11.995974448465169	0	11.780212333335189	0
0.2	11.991669406884018	0	11.821937321808754	0
0.4	11.984728394383922	0	11.859076458515744	0
0.6	11.974496498029186	0	11.905917027388661	0
0.8	11.960417930928731	0	11.931188450176629	0
1	11.942064600074023	0	11.942064600074023	0

Table 6. Comparison of the TBM with the exact solution for solving the discharging of a capacitor in Model 4.

α	TBM lower approximate solution	TBM absolute error	TBM upper approximate solution	TBM absolute error
0	0.0040255515348301	4.33680e-18	0.2197876666648101	8.32667e-17
0.2	0.0083305931159827	7.80626e-18	0.1780626781912458	8.32667e-17
0.4	0.0152716056160777	8.67317e-18	0.1409235414842563	1.94289e-16
0.6	0.0255035019708145	1.73723e-18	0.1085031902559575	2.22044e-16
0.8	0.0395820690712690	1.00834e-17	0.0808553639890256	8.32663e-17
1	0.0579353999259772	1.04834e-17	0.0579353999259772	1.52655e-16

The TBM with FIVP was successfully used to solve the crisp capacitor model, and the outcomes were compared with the exact solution. Tables 5 and 6 display the estimated outcomes of charging and discharging the capacitor, respectively. Figures 12–17 show the computed approximate solutions using the TBM developed in this study to illustrate the uncertain behavior of the charging and discharging capacitor model with various values of $\alpha \in [0,1]$. The tables show that the accuracy of the solution in terms of absolute error is very high.

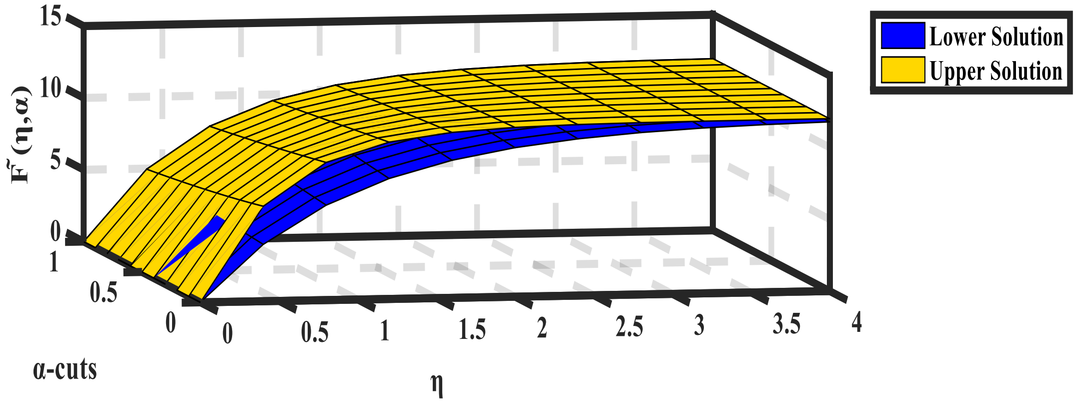

Figure 12. 3-Dimensional surface graph solution via the developed TBM for Model 4 with charging capacitor.

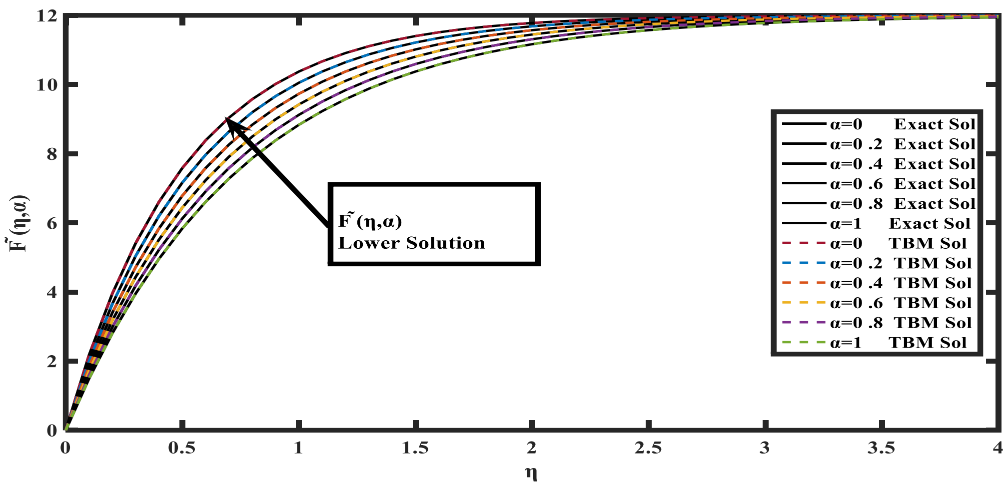

Figure 13. Uncertainty of Model 4 with α-cuts using TBM and a comparison with the exact solution.

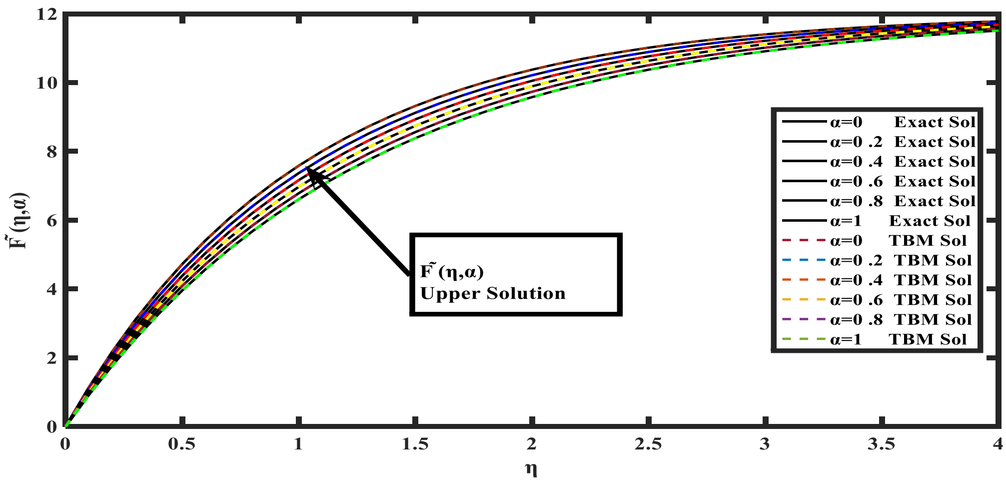

Figure 14. Uncertainty of Model 4 with α-cuts using TBM and a comparison with the exact solution.

The capacitor is fully charged when the uncertain parameter $\alpha = 0$; according with Figures 13 and 14, the solution (membership values with r-cuts) of the charging capacitor model in Eq (21) decreases with the lower bound and increases with the upper bound with the time interval [0,4]. In addition, the use of the triangular fuzzy number for the initial condition of the capacitor charging model ranges [2,4] for time. This gives more information for the approximate solution $\tilde{u}(x)$ of the model than the initial condition.

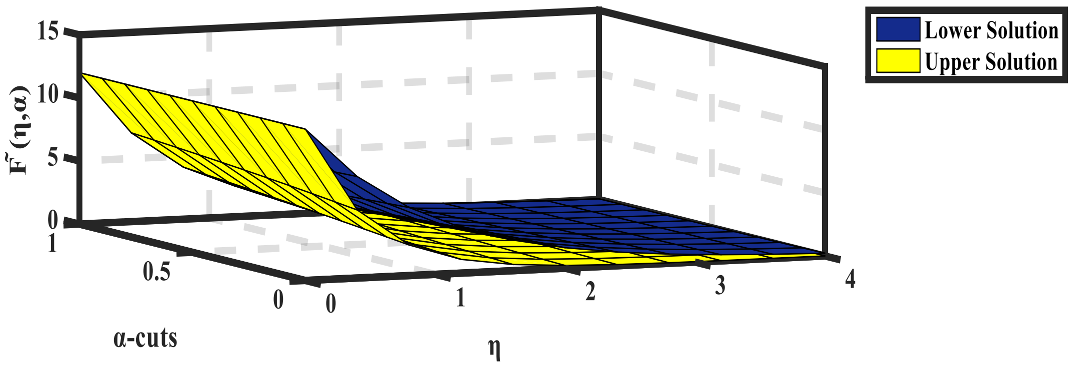

Figure 15. 3-Dimensional surface graph solution via the developed TBM for Model 4 with charging capacitor.

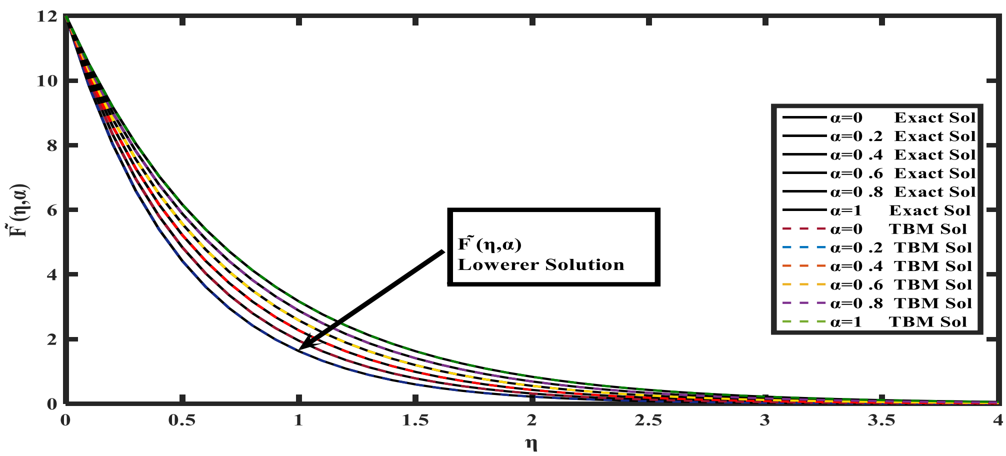

Figure 16. Uncertainty of Model 4 with α-cuts using TBM and a comparison with the exact solution.

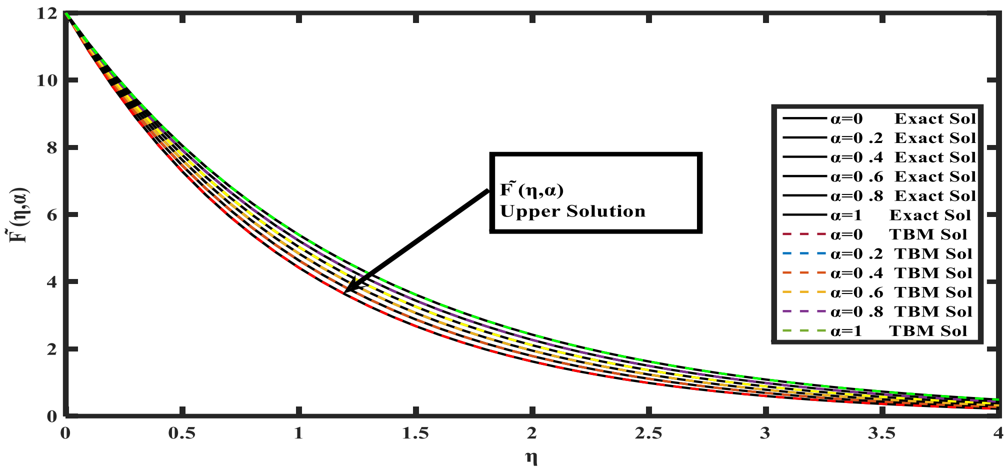

Figure 17. Uncertainty of Model 4 with α-cuts using TBM and a comparison with the exact solution.

The capacitor is fully discharged when the uncertain parameter $\alpha = 0$; according to Figures 16 and 17, the solution (membership values with r-cuts) of the discharging capacitor model in Eq (21) increases with the lower bound and decreases with the upper bound with the time interval [0,4]. In addition, the use of the triangular fuzzy number for the initial condition of the capacitor discharging model has a range of [2,4] for time. This gives more information for the approximate solution $\tilde{u}(t)$ of the model than the initial condition.

The graphs comparing the exact and approximate solutions demonstrate high accuracy, as the overlapping plots indicate the precision of the proposed method. Furthermore, the computation time (in seconds) required to obtain the approximate solutions for the numerical examples is presented in Table 7 below.

Table 7. Time taken to compute approximate solutions of the real-life models.

α	Model 1 time/s	Model 2 time/s	Model 3 time/s	Model 4 time/s
0	0.4767	0.4678	0.4768	0.4278
0.2	0.5673	0.4576	0.4626	0.4376
0.4	0.4602	0.4352	0.4342	0.4252
0.6	0.7021	0.4701	0.4521	0.4201
0.8	0.4423	0.4243	0.4253	0.4243
1	0.4200	0.4200	0.4200	0.4200
α	Model 1 time/s	Model 2 time/s	Model 3 time/s	Model 4 time/s
0	0.4767	0.4678	0.4768	0.4278
0.2	0.5673	0.4576	0.4626	0.4376
0.4	0.4602	0.4352	0.4342	0.4252
0.6	0.7021	0.4701	0.4521	0.4201
0.8	0.4423	0.4243	0.4253	0.4243
1	0.4200	0.4200	0.4200	0.4200

5. Conclusions

This study aimed to develop a numerical technique for solving first-order FIVPs with improved accuracy in absolute error. It utilized the Taylor series approach to develop TBMs with two fuzzy higher derivatives. The results showed superior accuracy of the TBM, demonstrating its zero-stable, absolutely stable, and convergence properties. The method was applied to real-life problems, solving various models with improved accuracy in absolute error. The fuzzy form of models allowed for easier analysis of uncertain behavior, making the methods developed viable approaches for solving FDEs. The study's findings suggest that fuzzy models can be used to analyze uncertain behavior, making them more accurate and feasible for real-world applications. At the end of this study, the developed method can be extended in future research to other types of differential equations, such as fuzzy fractional differential equations and fuzzy partial differential equations (PDEs).

Author contributions

Kashif Hussain: Writing − original draft, coding; Ala Amourah: Review and editing; Ali Fareed Jameel: Methodology and analysis; Jamal Salah: Funding; Nidal Anakira: Review and editing. All authors have read and approved the final version of the manuscript for publication.

Use of Generative-AI tools declaration

The authors declare that they have not used Artificial Intelligence (AI) tools in the creation of this article.

Conflict of interest

All authors declare no conflicts of interest in this paper

References

1. S. Abbasbandy, T. A. Viranloo, O. Lopez-Pouso, J. J. Nieto, Numerical methods for fuzzy differential inclusions, *Comput. Math. Appl.*, **48** (2004), 1633−1641. https://doi.org/10.1016/j.camwa.2004.03.009
2. O. Adeyeye, Z. Omar, Numerical solution of first order initial value problems using a self-starting implicit two-step Obrechkoff-type block method, *J. Math. Stat.*, **12** (2016), 127−134. https://doi.org/10.3844/jmssp.2016.127.134
3. N. B. Ahmad, J. Kavikumar, M. Mamat, A. Hamzah, N. Shamsidah, Fuzzy differential equations by using modified Romberg's method, *Prosiding Seminar Kebangsaan Aplikasi Sains dan Matematik*, **29** (2013), 51−64.
4. A. Ahmadian, S. Salahshour, C. S. Chan, D. Baleanu, Numerical solutions of fuzzy differential equations by an efficient Runge–Kutta method with generalized differentiability, *Fuzzy Set. Syst.*, **33** (2018), 47−67. https://doi.org/10.1016/j.fss.2016.11.013

5. N. Ahmady, T. Allahviranloo, E. Ahmady, A modified Euler method for solving fuzzy differential equations under generalized differentiability, *Comput. Appl. Math.*, **39** (2020), 1−21. https://doi.org/10.1007/s40314-020-1112-1
6. T. Allahviranloo, S. Abbasbandy, N. Ahmady, E. Ahmady, Improved predictor-corrector method for solving fuzzy initial value problems, *Inform. Sci.*, **179** (2009), 945−955. https://doi.org/10.1016/j.ins.2008.11.030
7. F. Babakordi, T. Allahviranloo, A new method for solving fuzzy Bernoulli differential equation, *J. Math. Ext.*, **15** (2021), 1−20.
8. B. Bede, L. Stefanini, Generalized differentiability of fuzzy-valued functions, *Fuzzy Set. Syst.*, **230** (2013), 119−141. https://doi.org/10.1016/j.fss.2012.10.003
9. S. S. L. Chang, L. A. Zadeh, On fuzzy mapping and control, *IEEE T. Syst. Man Cy.*, **2** (1972), 30−34. https://doi.org/10.1109/TSMC.1972.5408553
10. T. K. Fook, Z. B. Ibrahim, Two points hybrid block method for solving first-order fuzzy differential equations, *J. Soft Comput. Appl.*, **20** (2016)), 45−53. https://doi.org/10.5899/2016/jsca-00083
11. H. A. Hashim, A. H. Shather, A. F. Jameel, A. Saaban, Numerical solution of first order nonlinear fuzzy initial value problems by six-stage fifth-order Runge Kutta method, *Int. J. Innov. Technol. Explor. Eng.*, **8** (2019), 166−170.
12. W. Hohenauer, Hohenauer-Physical modelling based on first order ODEs, *SIMIODE*, 2018, 1−22.
13. K. Hussain, O. Adeyeye, N. Ahmad, Higher derivative block method with generalized step length for solving first-order fuzzy initial value problems, *IIUM Eng. J.*, **24** (2023), 158−169. https://doi.org/10.31436/iiumej.v24i1.2380
14. K. Hussain, O. Adeyeye, N. Ahmad, Numerical solution of second order fuzzy ordinary differential equations using two-step block method with third and fourth derivatives, *J. Nigerian Soc. Phys. Sci.*, **5** (2023), 1087. https://doi.org/10.46481/jnsps.2023.1087
15. K. Hussain, O. Adeyeye, N. Ahmad, R. Bibi, Third-fourth derivative three-step block method for direct solution of second-order fuzzy ordinary differential equations, *IAENG Int. J. Comput. Sci.*, **49** (2022), 856−863.
16. S. Isa, Z. A. Majid, F. Ismail, F. Rabiei, Diagonally implicit multistep block method of order four for solving fuzzy differential equations using Seikkala derivatives, *Symmetry*, **10** (2018), 42−63. https://doi.org/10.3390/sym10020042
17. K. Ivaz, A. Khastan, J. J. Nieto, A numerical method for fuzzy differential equations and hybrid fuzzy differential equations, *Abstr. Appl. Anal.*, **3** (20133), 1−10. https://doi.org/10.1155/2013/735128
18. R. Jafari, W. Yu, X. Li, S. Razvarz, Numerical solution of fuzzy differential equations with Z-numbers using Bernstein neural networks, *Int. J. Comput. Intell. Syst.*, **10** (2017), 1226−1237. https://doi.org/10.2991/ijcis.10.1.81
19. M. K. Jain, S. R. K. Iyenger, *Numerical methods for scientific and engineering computation*, New Age International Limited Publication, 2007.
20. A. Jameel, N. R. Anakira, A. K. Alomari, I. Hashim, M. A. Shakhatreh, Numerical solution of n'th order fuzzy initial value problems by six stages, *J. Nonlinear Sci. Appl.*, **9** (2016), 627−640. https://doi.org/10.22436/jnsa.009.02.26
21. A. F. Jameel, A. I. M. Ismail, A. Sadeghi, Numerical solution of fuzzy IVP with trapezoidal and triangular fuzzy numbers by using the fifth-order Runge-Kutta method, *World Appl. Sci. J.*, **17** (2012), 1667−1674.

22. T. Jayakumar, K. Kanakarajan, Numerical solution for hybrid fuzzy system by improved Euler method, *Int. J. Appl. Math. Sci*., **6** (2012), 1847−1862.
23. K. Kanagarajan, M. Sambath, Runge-Kutta nystrom method of order three for solving fuzzy differential equations, *Comput. Meth. Appl. Math.*, **10** (2010), 195−203. https://doi.org/10.2478/cmam-2010-0011
24. M. Keshavarz, T. Allahviranloo, S. Abbasbandy, M. Modarressi, A study of fuzzy methods for solving systems of fuzzy differential equations, *New Math. Nat. Comput.*, **17** (2021), 1−27. https://doi.org/10.1142/S1793005721500010
25. M. Ma, M. Friedman, A. Kandel, Numerical solutions of fuzzy differential equations, *Fuzzy Set. Syst.*, **105** (1999), 133−138. https://doi.org/10.1016/S0165-0114(97)00233-9
26. F. H. Maghool, Z. H. Radhy, H. A. Mehdi, H. M. Abass, Simpson's rule to solve fuzzy differential equations, *Int. J. Adv. Res. Sci. Eng. Techno*., **6** (2019), 11306−11315.
27. S. Mehrkanoon, M. Suleiman, Z. Majid, Block method for numerical solution of fuzzy differential equations, *Int. Math. Forum*, **4** (2009), 2269−2280.
28. H. S. Najafi, F. R. Sasemasi, S. S. Roudkoli, S. F. Nodehi, Comparison of two methods for solving fuzzy differential equations based on Euler method and Zadeh's extension, *J. Math. Comput. Sci.*, **2** (2011), 295−306. https://doi.org/10.22436/jmcs.002.02.09
29. V. Nirmala, V. Parimala, P. Rajarajeswari, Application of Runge-Kutta method for finding multiple numerical solutions to intuitionistic fuzzy differential equations, *J. Phys.: Conf. Ser.*, **1139** (2018), 1−8. https://doi.org/10.1088/1742-6596/1139/1/012012
30. N. Parandin, Numerical solution of fuzzy differential equations of 2nd-order by Runge-Kutta method, *J. Math. Ext.*, **7** (2014), 47−62.
31. P. Prakash, V. Kalaiselvi, Numerical solutions of fuzzy differential equations by using hybrid methods, *Fuzzy Inf. Eng.*, **4** (2012), 445−455. https://doi.org/10.1007/s12543-012-0126-9
32. M. L. Puri, D. A. Ralescu, Differentials of fuzzy functions, *J. Math. Anal. Appl.*, **91** (1983), 552−558. https://doi.org/10.1016/0022-247X(83)90169-5
33. F. Rabiei, F. A. Hamid, M. M. Rashidi, F. Ismail, Numerical simulation of fuzzy differential equations using general linear method and B-series, *Adv. Mech. Eng.*, **9** (2017), 1−16. https://doi.org/10.1177/1687814017715419
34. P. Rajkumar, S. Rubanraj, Numerical solution of fuzzy differential equations by seventh order Runge-Kutta method, *J. Comput. Math. Sci.*, **10** (2019), 1518−1528. https://doi.org/10.29055/jcms/1143
35. A. Ramli, Z. A. Majid, *An implicit multistep block method for fuzzy differential equations*, In: 7th International Conference on Research and Educations in Mathematics (ICREM7), **107** (2015), 113−119. https://doi.org/10.1109/ICREM.2015.7357031
36. A. Ramli, Z. A. Majid, Fourth-order diagonally implicit multistep block method for solving fuzzy differential equations, *Int. J. Pure Appl. Math.*, **107** (2016), 635−660. https://doi.org/10.12732/ijpam.v107i3.12
37. M. M. Salih, Using predictor-corrector methods for solving fuzzy differential equations, *Discover. Math. (Menemui Matematik)*, **36** (2014), 9−17.
38. S. Seikkala, On the fuzzy initial value problem, *Fuzzy Set. Syst.*, **24** (1987), 319−330. https://doi.org/10.1016/0165-0114(87)90030-3
39. K. Sevindir, H. Cetinkaya, On numerical solutions of fuzzy differential equations, *Int. J. Dev. Res.*, **8** (2018), 22971−22979.

40. J. Shokri, Numerical solution of fuzzy differential equations, *Appl. Math. Sci.*, **45** (2007), 2231−2246.
41. T. Smita, S. Chakraverty, Euler-based new solution method for fuzzy initial value problems, *Int. J. Artif. Intell. Soft Comput.*, **4** (2014), 58−79. https://doi.org/10.1504/IJAISC.2014.059288
42. Z. T. Yassin, W. Al-Hayani, A. F. Jameel, A. Amourah, N. Anakira, Solving fuzzy system of Fredholm integro-differential equations of the second kind by using homotopy analysis method, *AIMS Math.*, **10** (2025), 1704−1740. https://doi.org/10.3934/math.2025078
43. I. S. Zawawi, Z. B. Ibrahim, M. Suleiman, Diagonally implicit block backward differentiation formulas for solving fuzzy differential equations, *AIP Conf. Proc.*, **1522** (2013), 681−687. https://doi.org/10.1063/1.4801191